

ADVANCED PHASE ANALYSIS OF RETINAL VIDEOS USING ECG

Jan Šíma, Andrea Němcová, Radim Kolář

Department of Biomedical Engineering, Faculty of Electrical Engineering and Communication,
Brno University of Technology, Brno, Czech Republic

Abstract

Spectral analysis is one way to further investigate retinal hemodynamics and vessel pulsation. Specifically, for the phase component of the spectrum of retinal videos, the significance in retinal analysis has not yet been fully defined. The aim of this study is to determine whether the value of phase is relevant in the classification of blood vessels (arteries and veins). Using electrocardiographic signals recorded simultaneously with retinal video, we can determine how the phase component of the video behaves with respect to the cardiac cycle. As part of the experiment, we measured the retinal video of the left eye of 13 healthy subjects. We found that the phase delay between the maximal pulsation of arteries and veins in the optic nerve head tissue is on average 9% of the actual cardiac period. For our data set, this corresponds to an average time delay of 80.22 ms. We conclude that this phase delay between pulsations of arteries and veins can help in the classification of vessels in the optic nerve head.

Keywords

retinal video, spectral phase analysis, photoplethysmography, electrocardiography

Introduction

One of the most challenging diagnoses in ophthalmology is the accurate detection of early glaucoma. The most common causes include high intraocular pressure and impaired retinal blood flow. Preventive examination of arterial and venous pulsation in the retina (to determine if changes have occurred over time) could aid in making a proper diagnosis [1, 2]. However, distinguishing between arteries and veins in fundus images remains difficult even today. Neural networks are commonly used, but the principles behind their classification of vessels are not fully understood [3].

The retina allows direct, non-invasive visualization of microvascular circulation, which is unique among human tissues. Pulsatile fluctuations caused by the cardiac cycle are therefore observable throughout the retina, particularly in the optic nerve head (ONH) and the peripapillary region. These pulsatile phenomena include venous pulsations, commonly known as spontaneous venous pulsations (SVP), arterial pulsations (encompassing changes in arterial diameter and curvature), and changes in light absorption at specific wavelengths due to microcapillary and vascular alterations (referred to as retinal photoplethysmography, PPG) [4, 5]. The pulsatile nature of these phenomena is primarily governed by the cardiac cycle. However, additional factors such as intraocular pressure and

cerebrospinal fluid pressure also contribute to and influence retinal pulsations.

In a previous study [5] by our team, only spectral analysis of retinal pulsations was performed using the amplitude part of the spectrum in retinal videos. Therefore, we decided to perform the analysis also in the phase spectral component of the newly measured retinal videos, while simultaneously acquiring the electrocardiographic (ECG) signal. The reason for this is to observe the pulsation of the vessels in the ONH during the cardiac cycle. Heart rate variability (HRV) influences pulsation and therefore the phase components of the retinal vasculature and ONH. This fact has already been addressed [6].

So far, no publication has been published describing the mentioned phase analysis of retinal videos. This paper presents a retinal video phase analysis approach for vessel classification and verifies its potential.

The main hypothesis is to determine whether the phases within the cardiac cycle differ in the ONH, arteries and veins. If so, another hypothesis is to see if this method could be used to classify retinal vessels.

Materials and Methods

Based on previous insights, this paper outlines a procedure for spectral phase analysis that reflects all mentioned pulsations. Considering how the phase in the

optical disc of the retina is influenced by numerous pulsations and pressures, it is necessary to measure also ECG signal. This can be considered as a signal, which triggers the retinal pulsations and makes the pulsation phase analysis more reliable.

Acquisition system

The acquisition system [4, 5] comprises of three main modules (Fig. 1):

1. Video-ophthalmoscope (VO): It captures retinal video of the ONH and peripapillary area with a field of view of $20^{\circ} \times 17^{\circ}$, corresponding to approximately 6×5 mm in the retina. The CMOS camera (UI-3060 Rev 2, USB 3.0, IDS Imaging Development Systems GmbH, Germany) operates at a frame rate of 25 fps, with a retinal illumination of $50 \mu\text{W}/\text{cm}^2$.

2. Biosignal acquisition unit: BiosignalsPlux (PLUX Wireless Biosignals S.A., Lisbon, Portugal): It is a 4-channel unit records three physiological signals—ECG, ear photoplethysmography (PPG), and respiratory activity. In this study, only the ECG signal was utilized, sampled at 1000 Hz.

3. Synchronization unit: This Arduino-based unit generates a trigger signal to synchronize camera frame acquisition. The rising edge of this signal triggers frame acquisition and is simultaneously recorded by the BiosignalsPlux unit. This synchronization ensures precise alignment of retinal video frames with recorded biosignals, facilitating accurate temporal correlation analysis.

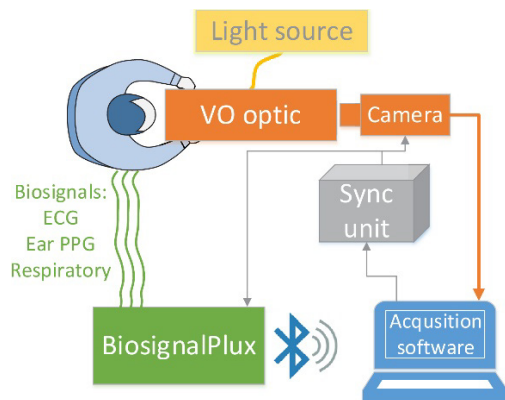


Fig. 1: Illustration of our proposed acquisition setup. Reprinted from [7], with permission.

Dataset

Thirteen healthy subjects were measured after pupil dilation (tropicamide drops, concentration of 0.25%). The measurement duration was 10–15 seconds. First, blood pressure (Omron, Intellisense, Japan) and intraocular pressure (Huvitz, tonometer HNT-1, South Korea) were measured. The fundus image was acquired with a clinical fundus camera (Canon CR-1, Canon EOS 40D, Japan). We used retinal illumination at a wavelength of 525 nm for the video-ophthalmoscope

measurements [7]. Light with this wavelength provides good contrast of the vessels compared to ONH.

This study followed the principles of the Declaration of Helsinki for research involving human subjects, and informed consent was obtained from all study participants. The measurement procedure was reviewed and approved by the Ethics Committee of Brno University of Technology (no. EK:03b/2021).

Data processing

This section describes the processing of measured data from the VO and BiosignalsPlux. The methodology for estimating blood volume changes based on the pulsating light intensity signal in the retinal video using Fourier spectra is described (Fig. 2). The preprocessing and detection of R waves in the ECG to determine cardiac cycles is also described. The individual steps are listed below:

a) R wave detection in ECG: The ECG signal was processed to detect the R-wave positions in each cardiac cycle. We proposed an automatic detection method, consisting of filtering and robust detection of local maxima. High frequency components were removed by lowpass FIR filter (cutoff frequency 20.00 Hz), and baseline was also removed by subtracting the low-frequency components obtained by lowpass IIR filter (cutoff frequency 0.67 Hz). A robust local maxima detector (function *findpeaks*) was then used to detect the R-wave.

b) Data synchronization: Similarly, the rising edges of the obtained synchronization square trigger signal were detected using the same local maxima detector, where the detector was applied to the first-order difference of this signal. A threshold half the size of the square wave with a minimum peak distance of 0.6 times the square wave period was applied. Simultaneous acquisition of biosignals and video allows us to determine the timing of each R-wave during video recording. Therefore, the frame corresponding to the R-wave position can be determined. It should be noted that due to different sampling frequencies for biosignals and video sequences, the exposure time of each frame (40 ms) corresponds to 40 samples in the ECG.

c) Alignment of frames: A previously published approach [8] was used to align each frame with respect to the first frame (i.e. reference frame). This approach corrects translational and rotational movements using a combination of phase correlation and tracking of blood vessel midlines.

d) Detection of distorted frames: Due to eye movements, which can occur during the exposure time of the frame, some frames may be blurred. Additionally, flickering artifacts cause significant distortion. These distorted frames cannot be restored and must be detected before analysis. The approach based on frame similarity with their neighbors was used; specifically, the Euclidean distance (ED) between each frame and the

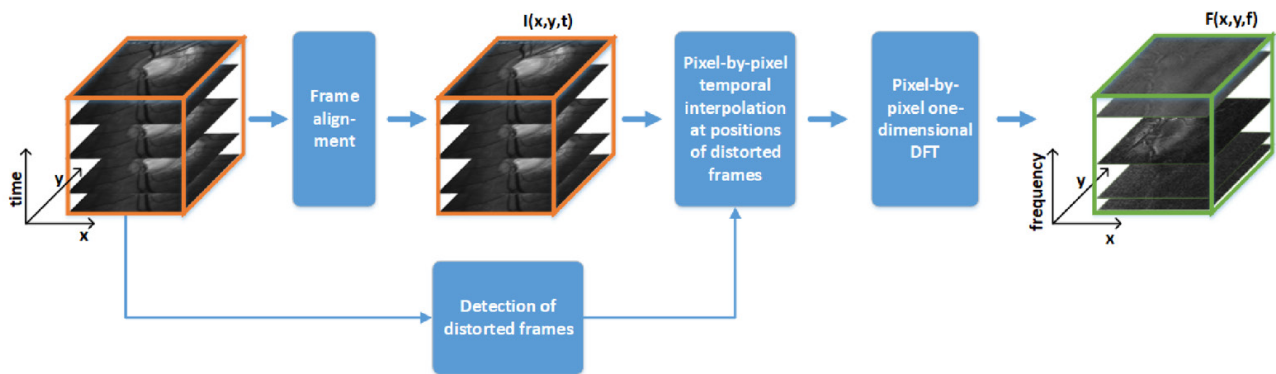


Fig. 2: The principle of the presented approach shows the main steps of the data processing—the acquired time stack is processed frame-by-frame to align the sequence; distorted frames are detected (providing indexes of frames); the temporal signals for each x, y position are Fourier transformed to the spectral domain (missing values due to distorted frames are temporally interpolated and spatial filter is applied on each frame before the Fourier transform). Reprinted from [4], with permission.

mean image from 71 surrounding frames was calculated and used for detecting distorted frames. From the ED, distorted frames were detected as outliers using the generalized extreme Studentized deviation test [9], where the most extreme ED values were removed until outliers were identified by the test.

e) Replacement of defective frames: Indexes of damaged frames (d) were used to interpolate corresponding pixel values over time from their neighbors (1D cubic interpolation).

f) Editing of the retinal video: For the sake of objectivity in evaluating the spectral phase component, the retinal video was always edited from the first to the last detected R-wave in the ECG recording.

g) Frequency analysis of retinal video: A pulsatile signal is a periodic signal driven by the heart rate frequency, which is defined by the first harmonic component.

Therefore, the transformation of a pulsating signal of relative intensity into the frequency domain allows estimating its spectral components, the amplitude $A(I)$ and the phase $\varphi(I)$ of the light intensity.

Consequently, the heart rate frequency (f_i) is determined as the position of the maximum amplitude in the spectral range, corresponding to the physiological values in the resting conditions: 50–100 beats per minute (bpm) (0.83–1.67 Hz).

The spectral space consists of two parts: the amplitude component and the phase component. Furthermore, we focused solely on the phase components, which should correspond to the temporal shifts between venous collapses and arterial pulsations, as described in the introduction. Thus, average phase values were computed based on segmented regions in the background of the ONH and in representative segments of the artery and vein. The ONH and vessel borders were created manually based on the fundus image. Monitored segments were manually labeled inside artery and vein based on anatomical knowledge, fundus image, and according to the work [10].

Heart rate variability analysis

For each subject, we computed ECG parameters: average R-R interval, the standard deviation of the R-R interval (SDNN) and the square root of the average of the squared differences between consecutive R-R intervals (rMSSD). We then compared these parameters with the phase values in the spectrum of the first harmonic component. The values are in Table 1.

Results

This chapter presents the results of the analysis of our dataset. Fig. 3 and Fig. 4 show an example of a cropped fundus image with the logarithmic amplitude spectrum at the frequency of the first harmonic component and cropped fundus image the phase spectrum at the frequency of the first harmonic component. Logarithms are used here only for better visualization.

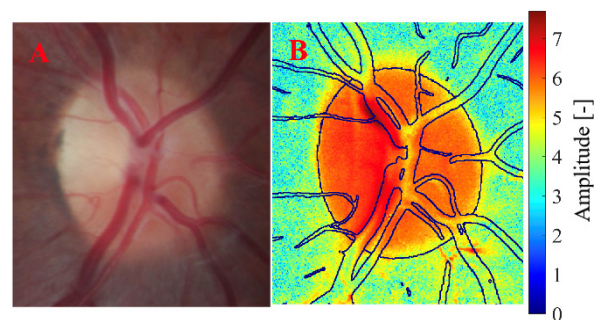


Fig. 3: A) Cropped fundus image. B) Logarithmic amplitude spectrum $A(I)$ at the frequency of the first harmonic component.

According to the annotated boundaries of the ONH and vessels, we could determine the exact boundaries of these structures in the spectrum. The boundaries of segmented vessels and the boundaries of the optic disc were overlaid onto Fig. 3 (B) and Fig. 4 (B). The algorithm for vessel segmentation and optic disc segmentation was previously developed [4].

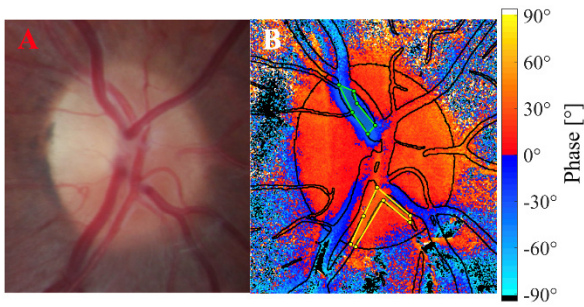


Fig. 4: A) Cropped fundus image. B) Phase spectrum $\phi(l)$ at the frequency of the first harmonic component with representative segment of artery (yellow) and vein (green).

A summary table was created from the computed phase parameters and heart rate variability analysis features. Furthermore, subject 4 was excluded from the analysis due to very low variability of the phase data. In Table 1, selected features of our analysis are presented: average phase values of absolute mutual differences between phases of ONH, arteries, and veins, average R-R interval, rMSSD and SDNN.

Table 1: The averages and standard deviations of selected features from the phase analysis.

Features	Average	Standard Deviation
Phase ONH–Artery (°)	9.87	9.45
Phase ONH–Vein (°)	31.18	12.96
Phase Artery–Vein (°)	31.76	13.31
R-R interval (ms)	892.57	168.16
rMSSD (ms)	39.34	24.21
SDNN (ms)	3.64	6.65

The absolute difference between the average phase values in the ONH and artery is 9.87° , between the ONH and vein is 31.18° and between the artery and vein is 31.76° .

Discussion

Phase values inside the ONH, arteries, and veins are both positive and negative across subjects. Nevertheless, the differences between these three analyzed compartments show a consistent trend. Based on the results, we believe that arterial pulsations are reflected in the ONH. This may be due to the extensive capillary network in the ONH background, where arterial pulsation predominates.

A limitation of the study is the small number of subjects and the low frame rate of the camera (25 fps). The frame rate is determined by the length of exposure required to ensure sufficient data quality (visible vessel pulsation). Higher light intensity is also uncomfortable for the subject. The length of the ECG for HRV analysis is also debatable, which we will try to increase

in the future. It should be noted that phase values are influenced by noise and eye movement artifacts.

Since this is the first publication of phase analysis of retinal videos, it is not possible to compare the results with other studies. Based on the results, phase analysis has potential in vessel classification and thus glaucoma assessment. Of course, much more extensive measurements are needed, including in glaucoma patients, to fulfil the potential of the analysis.

Conclusion

In the data, a significant difference in the average phase between arteries and veins is observed. Based on the phase values of the regions, it was calculated that the time difference between the maximum pulsation of arteries and veins in the ONH tissue is on average 9% of the current time. For our dataset, this corresponds to an average time delay of 80.22 ms. Similarly, a significant difference exists between the phases of the ONH background and veins. However, the phase difference between the ONH background and arteries is not very large. The first hypothesis has therefore been partially confirmed.

Thus, spectral phase analysis of retinal videos showed fairly consistent results in time delay between the main retinal arteries and veins in healthy subjects. This provides a good basis for further studies that will investigate the influence of retinal circulatory diseases (e.g. glaucoma). Since automatic recognition of retinal arteries and veins is still a big challenge for researchers, the results of this study may contribute to the development of an algorithm for retinal vessel classification. Based on the results of this study, classification of retinal vessels has potential, and the second hypothesis needs to be further tested which will require deeper research in this area.

Acknowledgement

The work has been supported by research grant No. 21-18578S of the Czech Science Foundation.

References

- [1] Shinde R. Glaucoma detection in retinal fundus images using U-Net and supervised machine learning algorithms. *Intelligence-Based Medicine*. 2021;5:100038. DOI: [10.1016/j.ibmed.2021.100038](https://doi.org/10.1016/j.ibmed.2021.100038)
- [2] Evans DW, Hosking SL, Embleton SJ, Morgan AJ, Bartlett JD. Spectral content of the intraocular pressure pulse wave: glaucoma patients versus normal subjects. *Graefes's Archive for Clinical and Experimental Ophthalmology*. 2002 May 28; 240(6):475–80. DOI: [10.1007/s00417-002-0460-4](https://doi.org/10.1007/s00417-002-0460-4)

- [3] Zhang J, Yang K, Shen Z, Sang S, Yuan Z, Hao R, et al. End-to-End Automatic Classification of Retinal Vessel Based on Generative Adversarial Networks with Improved U-Net. *Diagnostics*. 2023 Mar 17;13(6):1148. DOI: [10.3390/diagnostics13061148](https://doi.org/10.3390/diagnostics13061148)
- [4] Tornow RP, Odstreilík J, Kolar R. Time-resolved quantitative inter-eye comparison of cardiac cycle-induced blood volume changes in the human retina. *Biomedical Optics Express*. 2018 Nov 14;9(12):6237–54. DOI: [10.1364/boe.9.006237](https://doi.org/10.1364/boe.9.006237)
- [5] Kolar R, Odstreilík J, Tornow RP. Photoplethysmographic analysis of retinal videodata based on the Fourier domain approach. *Biomedical Optics Express*. 2021 Nov 9;12(12):7405–21. DOI: [10.1364/boe.441451](https://doi.org/10.1364/boe.441451)
- [6] Rosner B. Percentage points for a generalized ESD many-outlier procedure. *Technometrics*. 1983 May;25(2):165–72. DOI: [10.2307/1268549](https://doi.org/10.2307/1268549)
- [7] Kolar R, Vicar T, Chmelík J, Jakubíček R, Odstreilík J, Valterová E, et al. Assessment of retinal vein pulsation through video-ophthalmoscopy and simultaneous biosignals acquisition. *Biomedical Optics Express*. 2023 May 12;14(6):2645–57. DOI: [10.1364/BOE.486052](https://doi.org/10.1364/BOE.486052)
- [8] Kolar R, Vicar T, Odstreilík J, Valterová E, Skorkovská K, Kralík M, et al. Multispectral retinal video-ophthalmoscope with fiber optic illumination. *Journal of Biophotonics*. 2022 May 23;15(9):e202200094. DOI: [10.1002/jbio.202200094](https://doi.org/10.1002/jbio.202200094)
- [9] Hu Q, Abramoff MD, Garvin MK. Automated construction of arterial and venous trees in retinal images. *Journal of Medical Imaging*. 2015 Nov 19;2(4):044001. DOI: [10.1117/1.jmi.2.4.044001](https://doi.org/10.1117/1.jmi.2.4.044001)
- [10] Labounkova I, Labounek R, Kolar R, Tornow RP, Babbs CF, McClelland CM, et al. Heart rate and age modulate retinal pulsatile patterns. *Communications Biology*. 2022 Jun 14;5(1):582. DOI: [10.1038/s42003-022-03441-6](https://doi.org/10.1038/s42003-022-03441-6)

Ing. Jan Šíma
Department of Biomedical Engineering
Faculty of Electrical Engineering and Communication
Brno University of Technology
Technická 3058/10, CZ-616 00 Brno

E-mail: 211214@vut.cz
Phone: +420 731 043 189